

Confinement effects and polarization dependence of luminescence from monolayer-thick Ge quantum wells

Janos Olajos, Jesper Engvall, and Hermann G. Grimmeiss
Department of Solid State Physics, Lund University, Box 118, S-221 00 Lund, Sweden

Marcus Gail and Gerhard Abstreiter
Walter Schottky Institute, Technische Universität München, Am Coulombwall, D-8046 Garching, Federal Republic of Germany

Hartmut Presting and Horst Kibbel
Daimler-Benz Research Centre, D-7900 Ulm, Federal Republic of Germany
 (Received 8 November 1995; revised manuscript received 21 February 1996)

We have investigated the luminescence from monolayer-thick Ge quantum wells pseudomorphic to Si(100) substrates. The electronic structure of these quantum wells was investigated by uniaxial stress, and polarization- and temperature-dependent electroluminescence. By identifying the symmetry and origin of the wave functions involved in the optical transitions, it was found that both the confinement in the thin wells, as well as the interface between the wells and the surrounding material, play an important role for the emission. [S0163-1829(96)03524-2]

INTRODUCTION

The possibility of growing high-quality SiGe heterolayers pseudomorphic on a Si substrate has opened up many concepts for devices, such as heterojunction bipolar transistors,¹ IR detectors, and wave guides.² This, together with an increasing scientific interest, is one of the reasons for several investigations on the luminescence properties of Si_{1-x}Ge_x alloy quantum wells (QW's) with Ge contents of 10–40%.^{3,4} The luminescence properties of such thin alloy layers are by now well understood. They consist of a no-phonon line as well as different momentum-conserving phonon replicas. The energies of these luminescence features are lower than the Si band-gap energy, mainly due to the large compressive strain in the alloy layer. The current understanding of samples with high Ge content is, however, still rather limited partly due to the built-in elastic energy which limits the thickness that can be grown without generation of dislocations or three-dimensional growth. The maximum thickness for Ge contents above 50% is of the order of a few nanometers, and, for pure Ge, the maximum thickness is reported to be 4–6 ML.^{5–8} Systems of thin Ge monolayers pseudomorphic on Si therefore require monolayer-sharp interfaces. In structures which include multilayer sequences of different atomic species such as, e.g., Si and Ge, the situation is further complicated due to the segregation of Ge during growth. It is, however, possible to grow monolayer-sharp structures by molecular-beam-epitaxy (MBE) surfactant-assisted epitaxy.⁹

Optical properties of such structures are of interest for the following reasons: (1) In a QW of a few monolayers thickness, the transition energy is governed not only by the large strain which reduces the transition energy, but also by a comparably large confinement energy which shifts the transitions to higher energies. (2) Effects due to the random nature of alloys are not expected in the optical spectra, since these structures do not contain alloy layers. (3) Theoretical

predictions¹⁰ suggest that the electronic properties of such structures are greatly influenced by interfaces, and should therefore exhibit an enhanced optical transition probability for no-phonon transitions due to the scattering of electrons at the Si-Ge interface. We reported earlier^{11,12} on a preliminary study of luminescence properties in such systems, but additional experiments were necessary in order to determine the origin of the electronic states involved in the transitions.

To further increase our understanding of the luminescence properties, we have investigated the photoluminescence (PL) and electroluminescence (EL) of QW's consisting of nominally 2–4 ML of Ge grown pseudomorphically on Si, both in normal incidence and from polished edge surfaces perpendicular to the growth direction. Additional investigations were performed by studying the luminescence signals under uniaxial stress along the $\langle 110 \rangle$ crystallographic axis. Two luminescence lines originating from the structure were conclusively identified to arise from a no-phonon (NP) line and a TO-phonon replica. By examining the polarization dependence of the NP line, the symmetry of the intermediate state at $\Gamma_{15'c}$, over which the indirect transition occurs, was identified. When studying the effect of doping, the luminescence energies were found to be little affected by doping. We see, however, a large confinement shift of the band-gap energies depending on the thicknesses of the Ge layers. It was further observed that the confinement shift determines the quantum efficiency of the luminescence at room temperature.

EXPERIMENTAL DETAILS

The samples used in this study were grown on p^+ substrates in a MBE apparatus¹³ with elemental sources of Si, Ge, Sb, and B. The Si was evaporated from an e -gun evaporator, while the other sources were effusion cells. Details of the structures are presented in Table I. The samples consisted of two QW's of Ge, each of them with a thickness of 2–4 ML, separated by pure Si. In one set of samples (samples

TABLE I. List of samples which have been used in this study. The value m is the number of Ge monolayers, which is also indicated by the first digit of the sample label. n is the number of Si monolayers between the Ge wells. x is the Ge concentration in the surrounding alloy. The column ‘‘alloy cover’’ denotes whether the alloy of the previous column covers one or both sides of the QW structure. H is the separation of the QW structures. N_A is the p doping in the multiple-quantum-well structure. The last column gives the energy of the no-phonon EL emission.

Sample	m	n	x	Alloy cover	H (Si)	N_A (10^{18} cm^{-3})	NP energy (eV)
2A (B2818)	2	17	0.15	Single	40	5	1.026
2B (B2976)	2	20	0.15	Double	50	5	1.018
2C (B2975)	2	20	0.15	Double	50	10	1.021
3A (B2974)	3	20	0.15	Double	50	5	0.970
3B (B2943)	3	20	0.15	Double	50	10	0.984
4A (B2817)	4	17	0.20	Single	40	5	0.918
4C (B2977)	4	20	0.15	Double	50	1	0.935
4D (B2942)	4	20	0.15	Double	50	10	0.934

2A and 4A), the two Ge wells were separated by 17 ML of Si, and on one side clad by ten nanometers of a $\text{Si}_{1-x}\text{Ge}_x$ alloy layer. These double-QW structures were repeated ten times, separated by 40 nm of Si. The 40 nm of Si are expected to be sufficient for the QW structures to behave as isolated systems. The QW structure was then clad by an n -type alloy cap layer of 5% Ge to act as a waveguide for the light in the epilayer, and to provide a p - n junction for diode measurements.

In the other set of samples, the two Ge wells were separated by 20 ML of Si, and clad by alloy layers on both sides. The structures were separated by 50 nm of Si and the n -type waveguide layer consisted of 2.5% Ge. One example of these structures (sample 3B) is shown in the inset of Fig. 1.

Sharp interfaces were obtained by depositing 1 ML of Sb on top of the growing structure to prevent segregation of Ge. Though the spontaneous incorporation of Sb resulted in an n doping of about $8 \times 10^{17} \text{ cm}^{-3}$, the entire QW structure was still p type due to overcompensation with B of varying concentration in the range between 1×10^{18} and 1×10^{19} atoms/ cm^{-3} . Resulting from the high p doping, the injection efficiency of electrons into the quantum-well region is expected to be low. However, even for samples with the highest B concentration, the luminescence intensities have been large enough to study the EL properties of the QW's without greater difficulties.

Selected samples were investigated by double-crystal diffractometry (DCD), transmission electron microscopy (TEM), and x-ray triple-axis diffractometry. The rocking curve (RC) obtained from the DCD measurements fit simulated data, and a simulation with parameters close to the nominal values of the structure yields a RC that fits well to the experimental RC. The TEM micrographs showed excellent structural quality in terms of planarity and interface sharpness. From the DCD measurements it was seen that the perpendicular lattice constant of Ge QW's correspond to fully strained Ge. Furthermore, in a recent publication⁷ on the crossover between two- and three-dimensional growth of monolayers of Ge, where no surfactant was used during growth, it was seen that the energies of the NP lines from the Ge wells shift to higher energies due to the interdiffusion of Si and Ge at the well boundaries. All these findings clearly

show that the samples used in this study indeed consist of pure Ge wells with thicknesses deviating with a maximum of 10% from the nominal values. It is not possible from the TEM and PL investigations to exclude a slight interdiffusion in the absolute vicinity of the Ge wells (2–3 ML). It is, however, irrelevant for the scattering mechanisms that will be discussed below if the interface consists of one or a couple of monolayers.

The samples were processed into two types of diodes for electrical measurements: mesa diodes of varying diameters with optical windows for studies at normal incidence, and

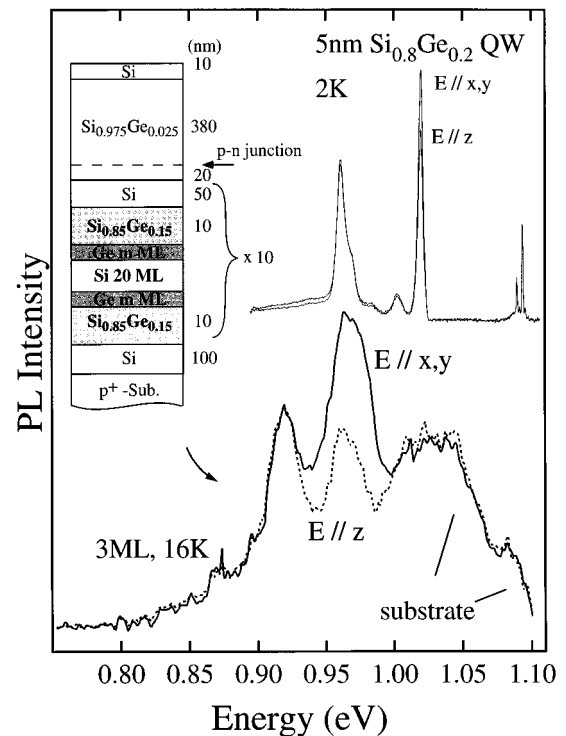


FIG. 1. PL spectra emitted with polarization in the plane of the epilayer (xy polarized) and in the growth direction (z polarized). The spectra in the upper part of the figure have been measured in a $\text{Si}_{0.8}\text{Ge}_{0.2}$ QW at 2 K, and the spectra in the lower part have been measured at 16 K on sample 3B, a 3-ML Ge QW sample. The inset shows the layer structure of sample 3B.

diodes of waveguide geometry used in polarization measurements. Samples with waveguides had most of the top surface metallized, and their lengths varied between 1 and 4 mm with lithographically defined stripe widths of 100 μm . The end $\langle 110 \rangle$ facets were mechanically polished.

PL measurements were performed on samples with polished end facets, but otherwise unprocessed. A BOMEM DA8 Fourier-transform spectrometer was used in the polarization measurements. Excitation in the PL experiments was provided by an Ar^+ -ion laser, and the luminescence was detected by LN_2 -cooled $\text{In}_x\text{Ga}_{1-x}\text{As}$ or North-coast Ge detectors. The polarization dependence was measured using a holographic grid polarizer on a CaF_2 substrate in front of the cryostat window.

RESULTS AND DISCUSSION

PL spectra of the 3-ML sample with the luminescence light polarized in the plane of the layer (xy polarized) and in the growth direction (z polarized) are shown in the lower half of Fig. 1. Due to the high doping, all bulk PL lines are broad, implying that different emission peaks overlap. Nevertheless, by comparing the emission of different samples with the luminescence signature of the substrate, an assignment of the different PL peaks to different layers has been possible. The peaks around 1.08 eV and the broad peak at 1.03 eV originate from the Si substrate as well as the SiGe cap layer, while the two peaks at 0.97 and 0.92 eV originate from the QW structure.¹¹ The high-energy peak from the QW showed a higher intensity for xy -polarized light than for z -polarized light, while the low-energy peak did not exhibit any polarization dependence at all. In our earlier communication,¹⁴ these two peaks were tentatively assigned to a no-phonon (NP) transition and a TO-phonon replica. A comparison of sample 3B with the polarization-dependent PL spectra of a $\text{Si}_{0.8}\text{Ge}_{0.2}$ alloy QW, which can be seen in the upper half of Fig. 1, indicates that mainly the Si-Ge TO vibration is present in the Ge-monolayer spectrum. This is reasonable considering that the structure is dominated by Si-Ge bonds at the spatial positions of the scattering potential, i.e., at the interfaces between Si and Ge. It is also seen that the polarization dependence of the alloy QW is virtually negligible. The NP line at 1.04 eV showed a slightly higher intensity for the $E//xy$ than for the $E//z$ polarization, but the difference is smaller than in sample 3B.

Our samples also exhibited a strong electroluminescence. EL spectra observed in samples 2B, 3A, and 4B, and measured with the electric-field vector parallel and perpendicular to the layers, are shown in Fig. 2. For these measurements, the edge-emitting structures were used. A considerable redshift of the luminescence is observed with increasing Ge layer thickness. Otherwise, the spectral features of the different samples are rather similar: The emission consists of two peaks separated by about 50 meV. The high-energy peak is mainly composed of xy -polarized light, while the low-energy peak is only slightly polarized. The apparent change in intensity of the low-energy peak observed for different polarization is probably due to a partial overlap of the two peaks.

In order to identify the transitions, the electronic states at the bottom of the valence and conduction bands have been

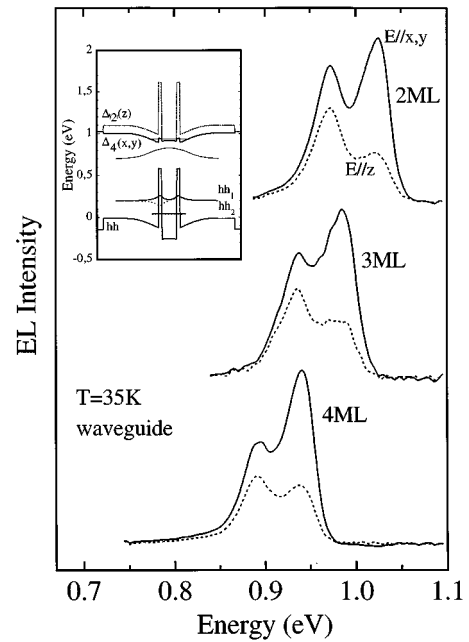


FIG. 2. Electroluminescence spectra for samples 2B, 3B, and 4C with 2-, 3-, and 4-ML Ge wells, respectively. The measurements have been performed by detecting light which has been polarized in the plane of the layer (xy polarized) as well as in the growth direction (z polarized). The inset shows results obtained from an effective-mass calculation using the structural parameters of sample 3B (see text).

modeled by an effective-mass approach where the valence-band offset and deformation potentials from Ref. 14 have been used. The calculated band diagram for the structures exhibited in the inset of Fig. 2 clearly shows that the main band offset is in the valence band. Although several bound states exist, only the two lowest bound heavy-hole states, $hh1$ and $hh2$, have been plotted. Due to the sign of the deformation potential for the valence band, the hh state of a structure pseudomorphic to Si is always higher in energy than the light-hole state. Due to the strain, the four equivalent Δ minima in the conduction band are split into a twofold set Δ_2 for the electron wave vector \mathbf{k} in the growth direction, and a fourfold set Δ_4 for \mathbf{k} in the plane of the QW. Whether or not the Δ_4 states are bound depends on the conduction-band alignment which is still under discussion.^{15,3} In either case, the offset is small, and the states therefore resemble bulk states of the barrier material. For Δ_2 states, the band offset is without any doubt type II due to the sign of the deformation potential. P doping may, however, transform both types of states into bound states, as the Coulomb attraction of holes in the QW's introduces a confining potential which results in a band bending.

Our calculations show that several different states may participate in the emission. In addition to the NP line and its TO replica, it is, for example, possible to anticipate transitions over the different types of conduction-band minima (twofold or fourfold, respectively), since it is expected that these electronic states should have approximately the same energy position. Furthermore, the $hh1$ and $lh1$ states in the valence band are energetically close when the confinement is taken into account. In order to examine the origin of the two

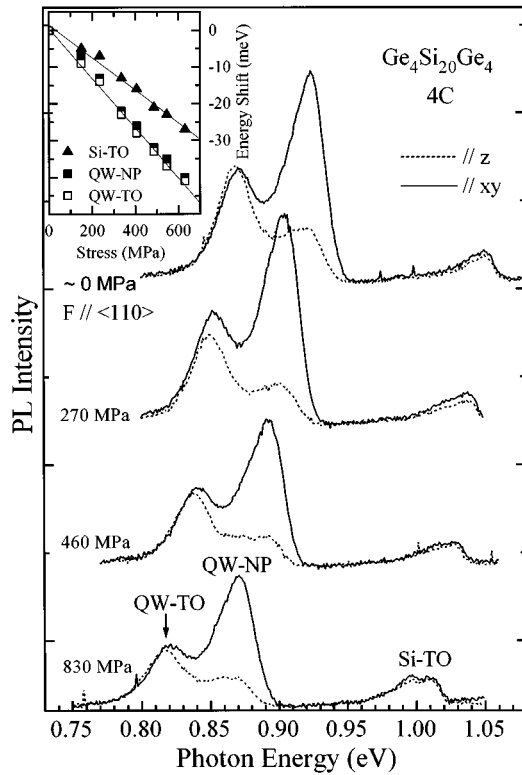


FIG. 3. Photoluminescence spectra as a function of uniaxial stress along the $\langle 110 \rangle$ direction. The inset shows the stress shift for the QW lines and the substrate line, respectively.

luminescence lines in more detail, and to investigate whether or not different electronic states are responsible for the two lines, additional experiments involving uniaxial stress and different temperatures were therefore carried out.

A distinction between the different cases is possible by performing uniaxial stress experiments, since the different conduction-band minima shift differently under applied external pressure, whereas the NP transition and its phonon replica are expected to shift with the same slope. Figure 3 shows results which have been obtained from an investigation of the PL spectra of sample 4C under uniaxial stress parallel with the $\langle 110 \rangle$ direction. It is readily seen that the two main peaks shift with similar slopes to lower energies as the applied stress is increased. The energy positions of the various peaks are plotted in the inset of Fig. 3, showing that the common shift of the two QW peaks is about -7.5 meV/kbar, i.e., about twice as large as for the Si-TO replica. Though a comprehensive theoretical analysis of the uniaxial stress behavior of the luminescence lines is beyond the scope of this paper, valuable information can nevertheless be gained from a brief discussion of the observed shift. The splitting of the conduction- and valence-band maxima in Si and Ge is well described by deformation potentials for small strains. For stress along the $\langle 110 \rangle$ direction, it is found that the x,y (in plane) conduction-band minima shift to lower energies by an amount $\Delta/3$, where Δ is the total-energy splitting between the xy and z valleys, respectively, in the absence of the built-in strain. In the valence band, external stresses will shift the heavy-hole valence band downwards and the light-hole band upwards in energy. These simple

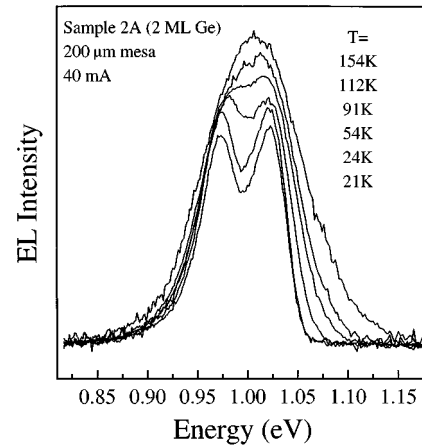


FIG. 4. EL spectra obtained at different temperatures from sample 2A with nominally 2-ML Ge wells and a B doping of $5 \times 10^{17} \text{ cm}^{-3}$. The spectra have been measured on a diode with a diameter of $200 \mu\text{m}$ and an injection current of 40 mA. The spectra are not plotted to the same scale in order to emphasize that the two lines maintain the same intensity relationship as the temperature is varied.

considerations, together with the magnitude of the observed shift, suggest that the luminescence we observe from the QW's originates from a NP transition and its phonon replica due to transitions between the xy conduction band and the heavy-hole valence band. It is also seen in Fig. 3 that the relative polarization ratios do not change with increasing uniaxial stress, an observation which additionally strengthens the assumption of a NP line and a TO replica.

The temperature dependence of EL for sample 2A with nominally 2-ML Ge wells and a doping of $5 \times 10^{17} \text{ cm}^{-3}$ is shown in Fig. 4. The spectra have been measured on a mesa diode with a diameter of $400 \mu\text{m}$ and an injection current of 40 mA. It is clearly seen that the ratio of the two peaks is rather constant in the energy range where the two peaks can be separated. If the peaks were due to different initial electronic states in thermal equilibrium, one would expect a temperature dependence of the ratio, reflecting the thermal distribution of the carriers in the two states. Since this is not the case, additional support is obtained for the hypothesis that the two peaks are a no-phonon line and a TO-phonon replica, arising from the same initial electronic state or from electronic states of similar energy.

The final energies and wave functions for these types of structures with only very thin Ge barriers are mainly given by the conduction-band edge of the surrounding $\text{Si}_{1-x}\text{Ge}_x$ alloy layers. The electronic wave functions observed in the transitions can therefore be modeled by using the symmetry properties of the bulk wave functions of biaxially compressed Si. A comprehensive study of the excitonic absorption properties of Si under uniaxial stress is, e.g., found in Ref. 16, where the authors studied the strain shifts and polarization selection rules for TO-phonon-assisted indirect transitions. The intensities for excitonic lines in optical spectra corresponding to TO-assisted indirect transitions between the $\Gamma_{25'} \text{ } \nu$ valence and $\Delta_{1,c}$ conduction bands are proportional to¹⁶

$$g = \left(\left| \frac{\langle \Gamma_{25',v} | \hat{e} \cdot \mathbf{p} | \Gamma_{15',c} \rangle \langle \Gamma_{15',c} | H_p | \Delta_{1,c} \rangle}{E(\Delta_{1,c}) - E(\Gamma_{15',c})} \right|^2 + \left| \frac{\langle \Gamma_{25',v} | H_p | \Delta_{5,v} \rangle \langle \Delta_{5,v} | \hat{e} \cdot \mathbf{p} | \Delta_{1,c} \rangle}{E(\Gamma_{25',v}) - E(\Delta_{5,v})} \right|^2 \right), \quad (1)$$

where \hat{e} is the unit polarization vector of the incident electric field, \mathbf{p} is the linear momentum of the electron, and H_p is the Hamiltonian for the electron-phonon interaction. The first term on the right-hand side of Eq. (1) is due to the contribution of indirect processes via the $\Gamma_{15',c}$ conduction band as an intermediate state, while the second right-hand term is the contribution of indirect transitions via the $\Delta_{5,v}$ valence-band intermediate state. It was found, both experimentally and theoretically, that the only symmetry-forbidden transition in the stress spectra is the transition between the hh ($|\frac{3}{2}, \frac{3}{2}\rangle$) valence band and the Δ_2 conduction band for light polarized with the electric-field vector perpendicular to the stress axis, i.e., $E//x,y$ in our notation. All other transitions are allowed for any polarization, and, specifically, the TO-assisted Δ_4 -hh transition is of equal magnitude for both polarizations.

The selection rules apply for TO-assisted transitions, and can be used in our case since, in principle, only TO phonons have been observed in the PL and EL spectra of Si/Ge microstructures. When studying the selection rules for NP lines, which in indirect semiconductors involves an intraband scattering in k space, one has to consider matrix elements between the basis function of the conduction and valence bands at the points in the Brillouin zone over which the NP transitions take place. In principle, only two points have to be considered, the Γ point and the point at the conduction-band minima. Furthermore, it is reasonable to assume that electrons are more affected by scattering processes in k space due to the Ge layers than the holes, since this is the case in Si and Ge.¹⁶ A set of unperturbed wave functions for [001] stress and holes at $\Gamma_{25'}$ can be chosen as¹⁷

$$\begin{aligned} |\frac{3}{2}, \frac{3}{2}\rangle_{001} &= \sqrt{\frac{1}{2}} |(X+iY)\uparrow\rangle, \\ |\frac{3}{2}, \frac{1}{2}\rangle_{001} &= \sqrt{\frac{1}{6}} |[2Z\uparrow + (X+iY)\downarrow]\rangle, \\ |\frac{1}{2}, \frac{1}{2}\rangle_{001} &= \sqrt{\frac{1}{3}} |[Z\downarrow - (X+iY)\downarrow]\rangle, \end{aligned} \quad (2)$$

where X , Y , and Z are the valence-band wave functions which transform as atomic p functions under the operations of the T_d group, and \uparrow and \downarrow indicate spin-up and spin-down, respectively, referring to the stress axis. If one chooses x , y , and z as basis functions of the $\Gamma_{15',c}$ conduction band, it has been shown¹⁸ that the only nonzero matrix elements of $\hat{e} \cdot \mathbf{p}$ between $\Gamma_{25',v}$ and $\Gamma_{15',c}$ are given by

$$\begin{aligned} \langle X|p_y|z\rangle &= \langle Z|p_y|x\rangle = \langle Y|p_z|x\rangle, \\ \langle X|p_z|y\rangle &= \langle Z|p_x|y\rangle = \langle Y|p_x|z\rangle \neq 0. \end{aligned} \quad (3)$$

The outcome of this discussion is summarized in Fig. 5, where all allowed optical transitions for both the NP lines and TO replicas are shown. Since the TO replica in our spectra has always been observed with similar intensity, independent of polarization (see Figs. 1, 2, and 3), we conclude that the TO lines originate mainly from transitions between hh

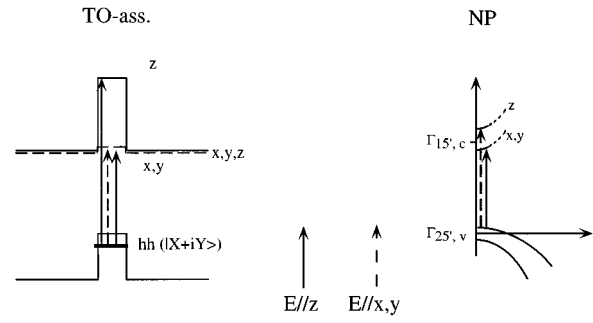


FIG. 5. Band lineup as obtained from our calculation. The arrows indicate different interband transitions. The polarization of the light is labeled for different transitions.

states and xy conduction-band states, as exhibited in Fig. 5. It is also noticed that the NP transition with in-plane polarized light ($E//x,y$) is only allowed to z components in the conduction band. Since the NP line of all luminescence spectra measured in our Ge-monolayer samples is mainly observed with $E//xy$, we believe that this transition occurs from the hh-hole valence subband over z components in the conduction band at $\Gamma_{15',c}$.

A comparison of the polarization-dependent PL spectra of a $\text{Si}_{1-x}\text{Ge}_x$ alloy quantum well (Fig. 1), with the Ge-monolayer samples reveals that the NP line in the alloy spectrum is essentially independent of polarization. This difference can be understood if one considers the possible mechanisms for the NP line in the two different cases. It is generally believed that the random-alloy scattering in an alloy QW gives rise to the breakdown of selection rules for indirect transitions. This scattering is, however, totally isotropic and does not introduce a preference in the symmetry of the final states in the scattering process. In the case of Ge-monolayer samples, it is reasonable to assume that the scattering due to the Si-Ge interface is highly anisotropic. For xy electrons, moving in the plane of the QW, the scattering potential is mainly a result of the Si-Ge bonds between the two different layers. The experimental observation that only electrons of z symmetry at the zone center participate in the NP line can be understood in terms of scattering of the x,y electrons by the Si-Ge bonds perpendicular to the plane of the quantum wells.

In addition to the polarization selection rules, the energy shift due to the confinement variation caused by the number of ML's of Ge is another important observation (Fig. 2). It has been observed earlier that the confinement has considerable consequences for the temperature dependence of the recombination processes at higher temperatures. The temperature dependence of the photoluminescence was studied in a previous publication,¹¹ where the decrease in PL intensity at higher temperatures was found to be due to the thermalization of trapped carriers out of the QW's. The temperature dependence is well described by the formula

$$I = I_0(1 + g e^{E_a/kT})^{-1}, \quad (4)$$

with an activation energy (E_a) close to the hole confinement energy. The intensity of the EL, which goes through a maximum at a temperature of about 100 K, has a temperature dependence slightly different from the PL. The decrease in

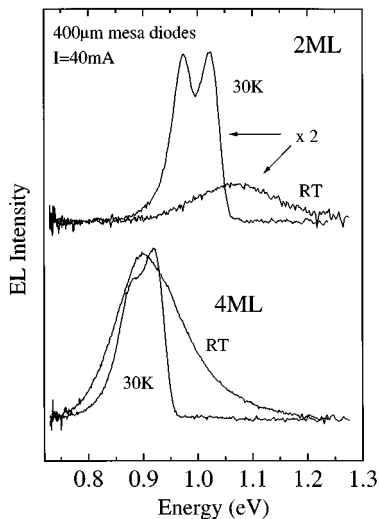


FIG. 6. Electroluminescence spectra of sample 2A with 2-ML Ge wells (top) and sample 4A with 4-ML Ge wells (bottom) which have been measured at 30 K and room temperature (RT), respectively. The spectra have been obtained from mesa diodes with a diameter of 400 μm , and 40-mA injection current.

intensity below 100 K is very similar for all samples, and is not fully understood. It should, however, be kept in mind that the sample has a thick cap layer that is relatively low doped. The freeze-out occurring in this layer can therefore shift more of the recombination to this part of the sample. In the range 100–300 K, a thermalization very similar to the PL behavior is seen in EL. The difference in confinement energies determines therefore the room-temperature EL behavior. In Fig. 6, an EL spectrum measured at 30 K is compared

with the room-temperature (RT) spectrum of a 2-ML sample (sample 2A) and a 4-ML sample (sample 4A). The integrated intensity of the 4-ML sample at RT is actually greater than at 30 K, and the decrease in luminescence when going from 77 K to RT is only about 30%. For the 2-ML sample, the decrease in intensity is much larger. At room temperature, the QW luminescence disappears, and only a peak at higher energy (1.05 eV) is observed, which is probably because of recombination in the barrier material since the carriers are less bound in the well due to the large confinement shift. The 3-ML samples display an intermediate situation where the EL at room temperature is composed of emission both from the barriers and the wells.

CONCLUSION

We have investigated the luminescence properties of ultrathin Ge QW's pseudomorphic to Si, and found that the luminescence energy, which is only weakly dependent on doping, is strongly effected by the thickness of the Ge layer. The thickness therefore indirectly determines the room-temperature EL efficiency in diodes. Stress and temperature dependence allow us to assign the NP line and the TO replica to the same electronic Δ_4 -hh transitions. The polarization dependence of the two lines demonstrates the importance of interfaces for the scattering process.

ACKNOWLEDGMENTS

This work was carried out within the European Basic Research Program (ESPRIT) under Contract No. P7128. The authors acknowledge financial support from the Swedish National Science Council, The Swedish Board for Technical Development, and the Bank of Sweden Tercentenary Foundation.

- ¹D.-X. Xu, G.-D. Shen, M. Wilander, W.-X. Ni, and G. V. Hansson, *Appl. Phys. Lett.* **52**, 2239 (1988).
- ²A. Splett, T. Zinke, K. Petermann, E. Kasper, H. Kibbel, and H. Presting, *IEEE Photon. Technol. Lett.* **6**, 59 (1994).
- ³N. L. Rowell, J.-P. Noël, D. C. Houghton, A. Wang, L. C. Lenchyshyn, M. L. W. Thewalt, and D. D. Perovic, *J. Appl. Phys.* **74**, 2790 (1993).
- ⁴S. Fukatsu, *Solid State Electron.* **37**, 817 (1994).
- ⁵J. Tersoff, *Phys. Rev. B* **43**, 9377 (1991).
- ⁶J. Bevk, J. P. Mannaerts, L. C. Feldman, B. A. Davidson, and A. Ourmazd, *Appl. Phys. Lett.* **49**, 268 (1986).
- ⁷P. Schittenhelm, M. Gail, J. Brunner, J. F. Nützel, and G. Abstreiter, *Appl. Phys. Lett.* **67**, 1292 (1995).
- ⁸T. P. Pearsall, J. Bevk, J. C. Bean, J. Bonar, J. P. Mannaerts, and A. Ourmazd, *Phys. Rev. B* **39**, 3741 (1989).
- ⁹M. Copel, M. C. Reuter, M. Horn von Hoegen, and R. M. Tromp, *Phys. Rev. B* **42**, 11 682 (1990).
- ¹⁰R. J. Turton and M. Jaros, *Mater. Sci. Eng. B* **7**, 37 (1990).
- ¹¹J. Engvall, J. Olajos, H. G. Grimmeiss, H. Kibbel, and H. Presting, *Phys. Rev. B* **51**, 2001 (1995).
- ¹²M. Gail, G. Abstreiter, J. Olajos, J. Engvall, H. Grimmeiss, H. Kibbel, and H. Presting, *Appl. Phys. Lett.* **66**, 2978 (1995).
- ¹³E. Kasper, H. Kibbel, and H. Presting, *Thin Solid Films* **183**, 87 (1989).
- ¹⁴C. G. Van de Walle and R. M. Martin, *Phys. Rev. B* **34**, 5621 (1986).
- ¹⁵T. Baier, U. Mantz, K. Thonke, R. Sauer, F. Schäffler, and H.-J. Herzog, in *Proceedings of the 22nd International Conference on the Physics of Semiconductors, Vancouver, Canada, 1994*, edited by D. J. Lockwood (World Scientific, Singapore, 1995), Vol. 2, p. 1568.
- ¹⁶L. D. Laude, F. H. Pollak, and M. Cardona, *Phys. Rev. B* **3**, 2623 (1971).
- ¹⁷M. Cardona and F. H. Pollak, *Phys. Rev.* **172**, 815 (1968).
- ¹⁸M. Cardona and F. H. Pollak, *Phys. Rev.* **142**, 530 (1966).